Polar Geosci., **16**, 1–21, 2003

Seismic refraction and wide-angle reflection exploration by JARE-43 on Mizuho Plateau, East Antarctica

Hiroki Miyamachi[1], Shigeru Toda[2], Takeshi Matsushima[3], Masamitsu Takada[4], Atsushi Watanabe[5], Mikiya Yamashita[6] and Masaki Kanao[7]

[1] *Department of Earth and Environmental Sciences, Faculty of Science, Kagoshima University, Kourimoto 1-chome, Kagoshima 890-0065*
[2] *Department of Earth Sciences, Faculty of Education, Aichi University of Education, Kariya 448-8542*
[3] *Institute of Seismology and Volcanology, Faculty of Sciences, Kyushu University, Shinyama, Shimabara 855-0843*
[4] *Institute of Seismology and Volcanology, Graduate School of Science, Hokkaido University, Kita-10, Minami-8, Kita-ku, Sapporo 060-0810*
[5] *Department of Earth and Planetary Sciences, Graduate School of Sciences, Kyushu University, Hakozaki 6-chome, Fukuoka 812-8581*
[6] *Department of Polar Science, The Graduate University for Advanced Studies, Kaga 1-chome, Itabashi-ku, Tokyo 173-8515*
[7] *National Institute of Polar Research, Kaga 1-chome, Itabashi-ku, Tokyo 173-8515*

(Received February 17, 2003; Accepted May 2, 2003)

Abstract: The 43rd Japanese Antarctic Research Expedition (JARE-43) carried out seismic exploration experiments on Mizuho Plateau, East Antarctica, in the austral summer season of 2001–2002. The exploration was composed of seven large explosions and 161 seismic stations distributed along the 151 km-long seismic line. The first arrival time data are analyzed by a refraction method. It is found that the ice sheet is composed of two layers: the upper layer with *P* wave velocity of 2.7–2.9 km/s has thickness of 35–45 m, and the lower layer with *P* wave velocity of 3.7–3.9 km/s continues to the bedrock. Lateral velocity variation in the upper-most crust is revealed: *P* wave velocity for the upper-most crust in the southern and central parts is 6.1–6.2 km/s and that in the northern part is 5.9 km/s. This result implies that the geological boundary observed along the coast in the Lützow-Holm Bay and Prince Olav Coast regions possibly continues to the inland area. The *S* wave velocity is also obtained to be roughly 3.5 km/s for the whole upper-most crust. Travel time analysis of two distinct reflection phases shows two horizontal reflecting planes located at 19 and 40 km depth; the latter corresponds to the Moho discontinuity.

key words: velocity model, Antarctica, Mizuho Plateau, crust

1. Introduction

The Japanese Antarctic Research Expedition (JARE) has studied the Enderby Land and Dronning Maud Land areas, East Antarctica, geologically and geophysically since 1958. Continuing geologic surveys have revealed that Enderby Land is composed of the Archaean Napier and late Proterozoic Rayner Complexes, and Eastern Dronning

Maud Land also includes the early Paleozoic Lützow-Holm and Yamato-Belgica Complexes. In particular, it is revealed that the Lützow-Holm Complex experienced igneous interaction in 550 Ma and had a varied metamorphic history originated from an early Paleozoic continent-continent collision (Hiroi *et al.,* 1991; Shiraishi *et al.,* 1994).

The thick ice sheet, however, prevents geological field activities in the inland areas. Therefore, geophysical approaches such as seismic, gravity and geomagnetic surveys are required to estimate the crustal structure in detail. The first seismic exploration was conducted along the Mizuho route in the Lützow-Holm Complex region by JARE-20, -21 and -22, in order to estimate the deep crustal structure (Ikami *et al.,* 1984; Ito and Ikami, 1984; Ikami and Ito, 1986). In spite of sparse station distribution, these studies showed a crustal thickness of about 40 km and the rough estimate of *P* wave velocity distribution in the crust.

Recently, a plan for the Structure and Evolution of East Antarctic Lithosphere (SEAL) transect project was proposed by Kanao (2001), in order to study the structure of the lithosphere beneath Enderby Land, and to understand the more detailed geological and geophysical evolution of this region. Following this project, JARE-41 seismic exploration with dense distribution of seismic stations was successfully carried out in 1999–2000 austral summer along the same Mizuho route as that by JARE-21 and -22 (Fig. 1). Details of the exploration have been reported in Miyamachi *et al.* (2001) and the velocity model was estimated by Tsutsui *et al.* (2001a, b). The model presents the significant fact that the Moho discontinuity is inclined from inland to the coast: its depth is 42 km at S-6 in Fig. 1 and 29 km at S-1. The *P* wave velocities for the ice sheet and upper-most crust are estimated accurately to be 3.8 and 6.2 km/s, respectively.

Following the JARE-41 exploration, JARE-43 carried out seismic exploration along a seismic line oblique to the JARE-41 seismic line to estimate the two-dimensional cross section of the crustal structure (Fig. 1). Details of this operation are described in Miyamachi *et al.* (2003). In this paper, we show the results of the refraction and wide-angle reflection analysis, and present the velocity model.

2. Seismic exploration and data acquisition

2.1. Seismic exploration

Seismic exploration in JARE-43 was performed on the Mizuho Plateau, during 48 days in the austral summer season of 2001–2002. This exploration consisted of seven large shots (SP1–SP7) with 700 kg charges, and one small shot (SP8) of 20 kg charges. A total of 161 temporary seismic stations were located along the 151 km-long seismic line, as shown in Fig. 1. This line crosses the JARE-41 seismic line at the H176 site (Miyamachi *et al.,* 2001) along the Mizuho route. The surface elevation along the line ranges from 1350 to 1550 m, as presented in Fig. 2. Station spacing was basically 1 km, but it was 500 m for a 10 km span in the central part. The coordinates of all stations and shot points were determined by applying the Global Positioning System (GPS) relative positioning method with the reference point installed temporarily at Syowa Station. They are listed in Miyamachi *et al.* (2003). Elevations of all stations in this paper are ellipsoidal heights on the WGS84 Ellipsoid.

Each station was equipped with a vertical seismometer with a natural frequency of

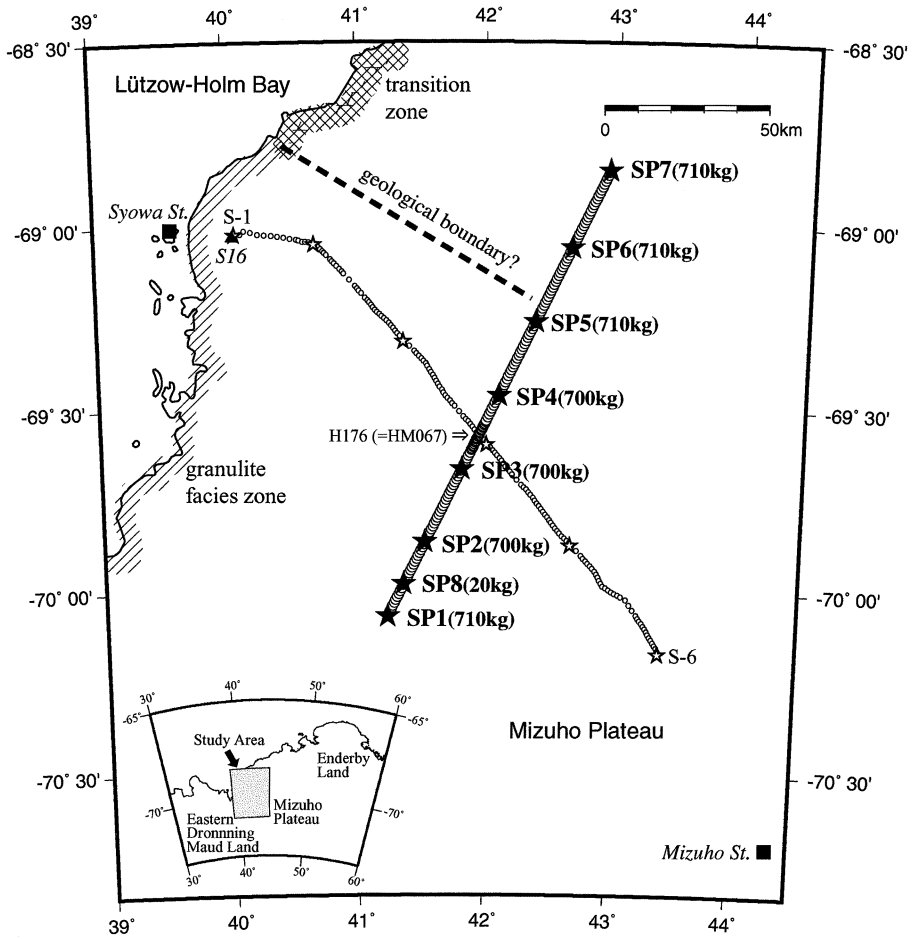

Fig. 1. Map showing the JARE-43 seismic line along the HM route. Solid and open stars are the shot locations by JARE-43 (this study) and by JARE-41, respectively. Large and small circles indicate the station locations in JARE-43 and in JARE-41, respectively. The crossing point between the Mizuho route (JARE-41) and the HM route (JARE-43) is marked as "H 176 (=HM067)". The number in kg beside each shot name is the weight of dynamite used.

2 Hz (model L-22D by Mark Products Co. Ltd.) and a portable and programmable digital recorder with a GPS clock (model LS8000SH with 20 Mbytes memory by Hakusan Corporation). A Cyclone battery (6V, 16Ah) was used as the power supply for the recorder. The seismometer with a 40 cm-long spike and the recorder with the battery in a plastic box were buried under the snow surface. The recorder automatically started the seismic observation after the time schedule assigned in advance, and wave data were sampled at 200 Hz, and stored in the memory.

We located additionally 5–6 extra seismic stations near each shot for a "line-up" observation in order to determine the precise *P* wave velocity profile of the ice sheet. Large shots with spacing of 25 km were fired in 25 m-deep holes drilled by a steam

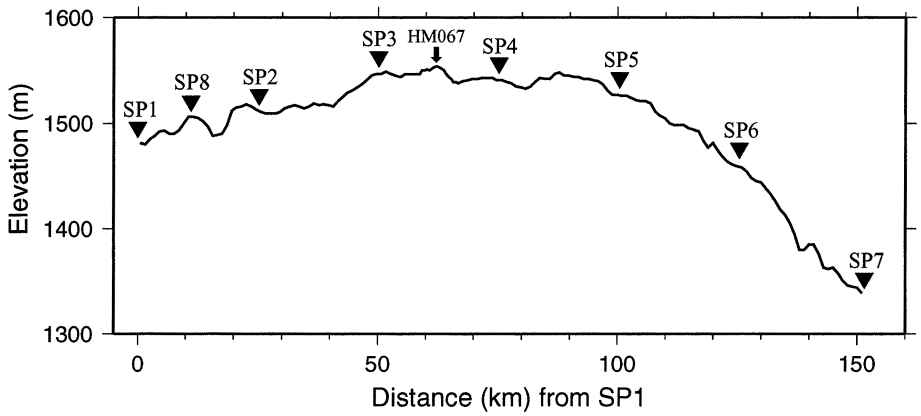

Fig. 2. Topographic profile along the JARE-43 seismic line (HM route). The elevations at all stations and shots are ellipsoidal heights on the WGS84 ellipsoid determined by the GPS relative-positioning. The station "HM067" is identical to the H176 point on the Mizuho route.

ejection-type drilling machine. After completing all shots, all seismic stations were recovered.

During our seismic exploration, we also carried out radio echo sounding in the northern and central parts of the seismic line (Takada *et al.,* 2002) and gravity measurements at the 151 seismic stations (Toda *et al.,* 2002), to estimate the thickness of the ice sheet and to infer the crustal structure from the gravity anomalies.

2.2. Seismic data

Figures 3–1 through 3–4 indicate record sections for SP1 to SP8. The ice sheet waves, labeled ***Ice Sheet***, traveling only through the ice sheet, the *S* waves, labeled ***S***, and the clearly dispersed surface waves, labeled ***Surface***, were observed. The first arrivals of all records, which were listed in Miyamachi *et al.* (2003), are shown in Figs. 4–1 to 4–3 after the reduction to 6.2 km/s velocity. The first arrivals are characterized by two branches. The first branch near all shot points corresponds to propagating waves inside the ice sheet. It gives almost the same apparent velocity of 3.8–3.9 km/s for the offset distance range of less than 10 km. In Fig. 5, we also show the travel time plots obtained by the line-up observations. The plots indicate that the ice sheet consists of two layers: 2.7–2.9 km/s for the upper layer and 3.7–3.9 km/s for the lower layer, respectively.

The second branch of the first arrivals corresponds to waves refracted through the upper crust just below the ice sheet. Clear onsets can be detected up to about 100 km offset distance for the shots except SP1. The apparent velocity in the southern and central parts seems to be 6.1–6.2 km/s. On the other hand, it is 5.8–6.0 km/s in the northern part, and the velocity boundary may be located between SP5 and SP6. We also found large local time delay for the range between SP3 and SP4. This may correspond to abrupt topographic change of the bedrock.

Though there is ambiguity whether the *S* wave is a ***PxS*** converted wave or generated from the explosion, we assume that *S* waves are radiated from the explosion and refracted through the upper crust. Figure 6 shows superposed travel time plots of *S* waves, which were reduced to 3.5 km/s for all shots. The large variation range of 1.0–

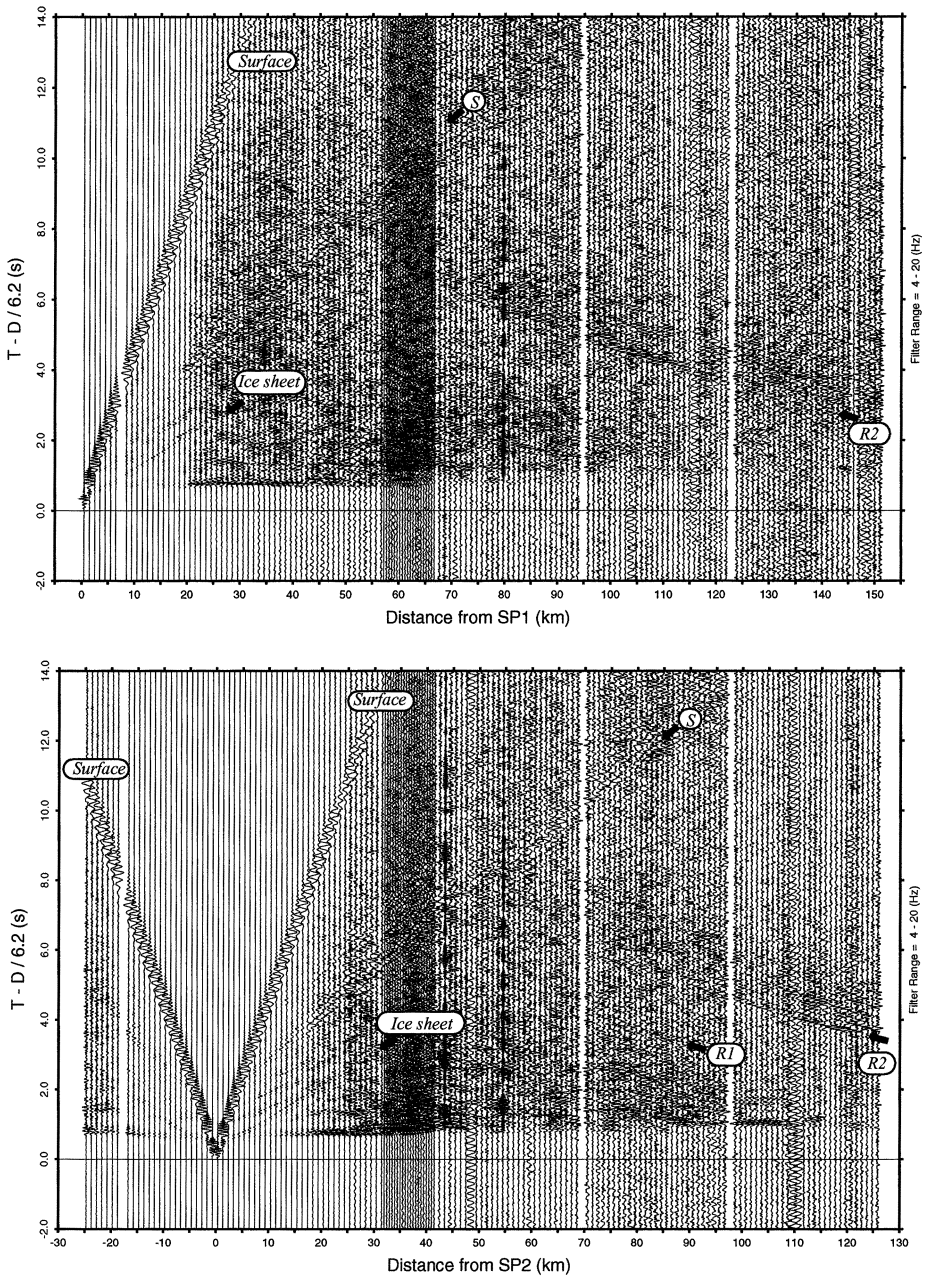

*Fig. 3–1. Record sections for SP1 and SP2. Each amplitude of the seismic wave is normalized by its maximum amplitude. "**R1**" and "**R2**" in the figures indicate the prominent later phases. "**Ice sheet**" means waves propagating only in the ice sheet. "**Surface**" means surface wave, while "**S**" is an S phase.*

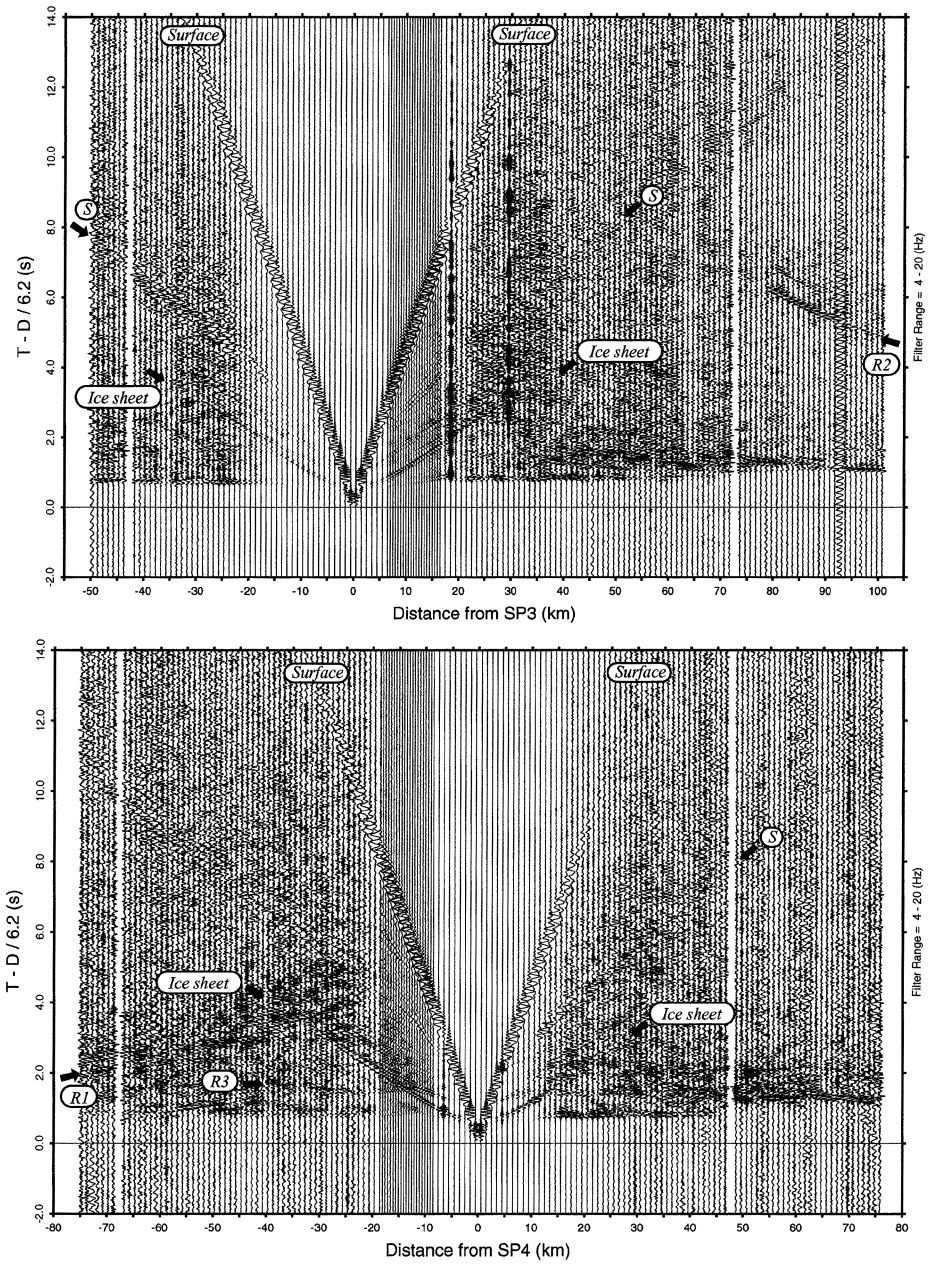

*Fig. 3–2. Similar record sections for SP3 and SP4. Explanations are the same as in Fig. 3–1, but we see another prominent phase, "**R3**", in the figures.*

2.0 s seen in the plots suggests large uncertainty of the velocity estimate.

Several distinct later phases are also identified. The phase labeled ***R1*** is observed for an offset distance from 30–90 km for SP2 and SP4. The other phase, labeled ***R2***, is widely observed over a distance range of 40–150 km for most of the shots. These later

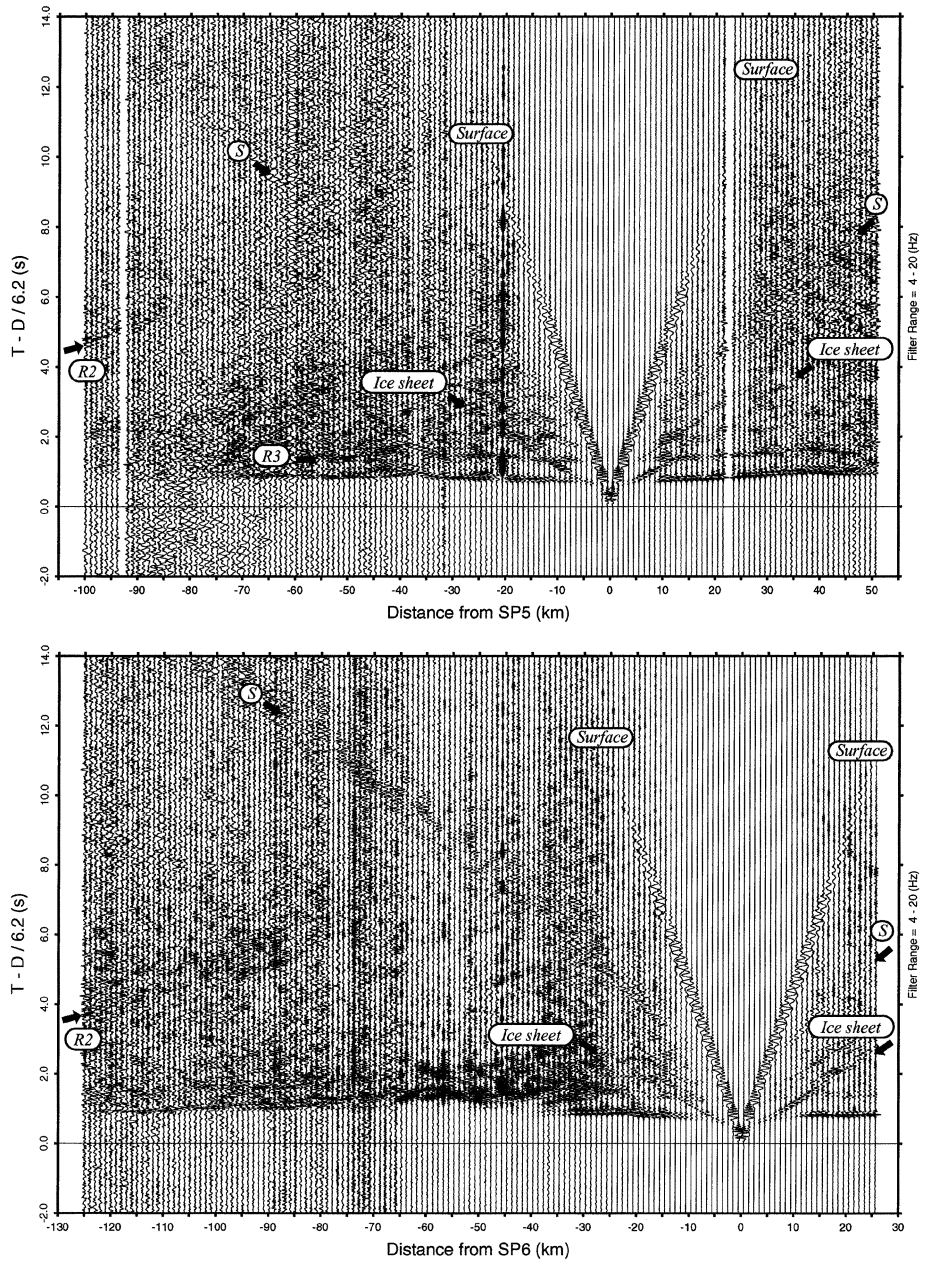

Fig. 3–3. Record sections for SP5 and SP6. Explanations are the same as in Fig. 3–1.

phases are considered as reflections with large amplitudes and will provide important information on the middle and lower crust. Another prominent phase, labeled ***R3***, which arrived after 0.6–0.7 s from the first onsets, is observed for SP4 and SP5. We can also observe some vibrations which probably originated from icequakes in record sections SP3, SP5 and SP6.

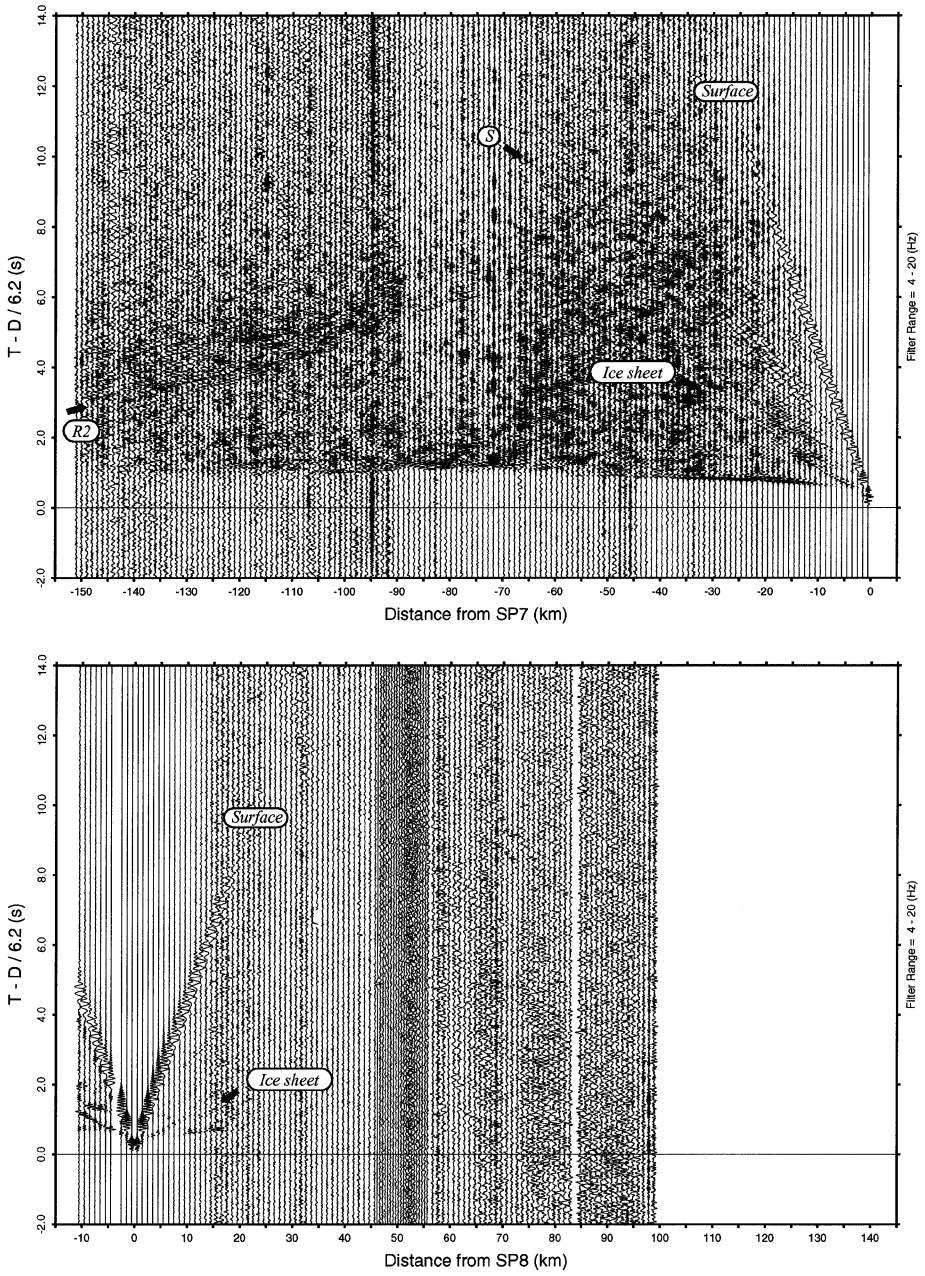

Fig. 3–4. Record sections for SP7 and SP8. Explanations are the same as in Fig. 3–1.

3. Travel time analysis and velocity modeling

3.1. P wave refraction analysis

Assuming a horizontally two-layered structure with the apparent velocities ob-

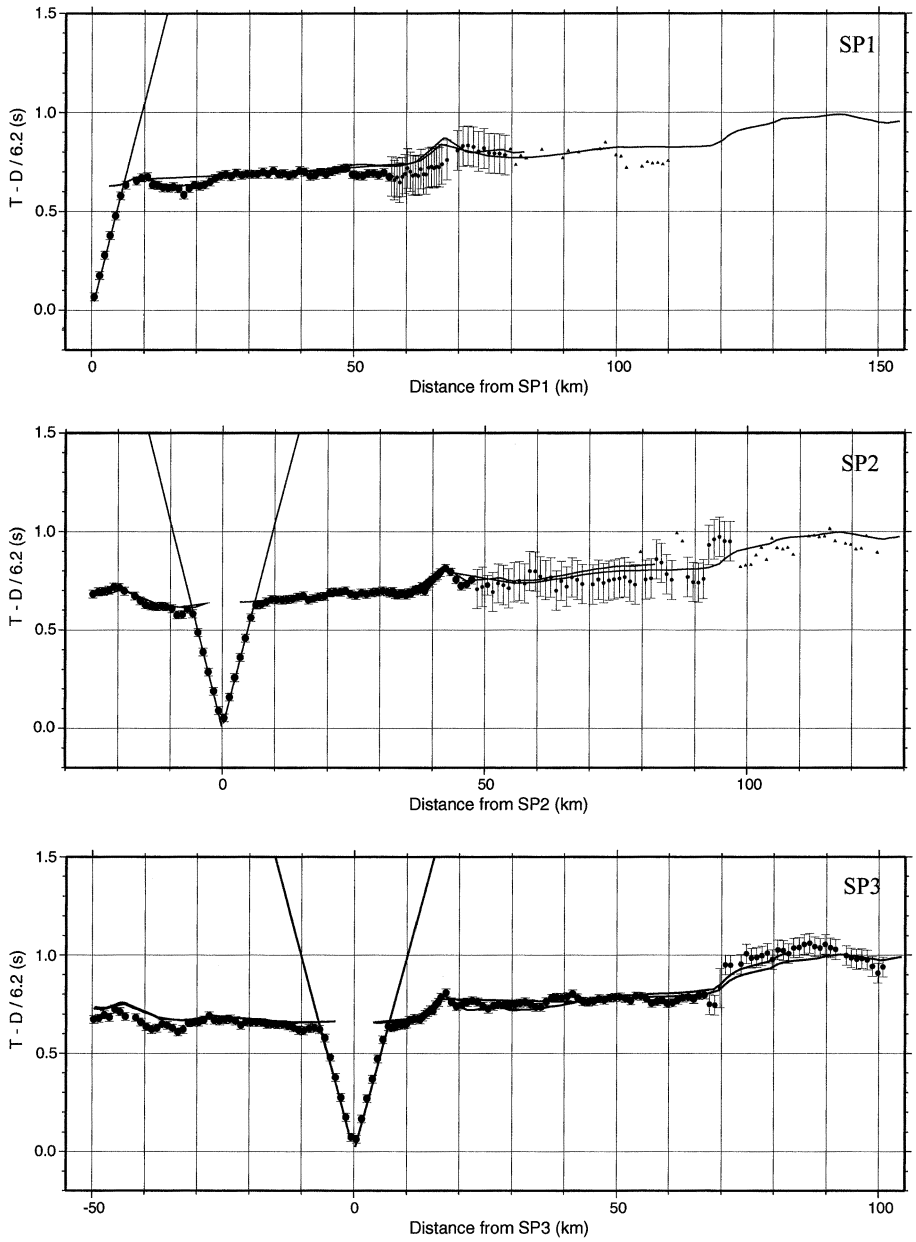

Fig. 4–1. P wave travel time plots reduced by the velocity of 6.2 km/s for SP1, SP2 and SP3. Solid circles with error bars indicate the observed travel times. Solid triangles are those for late arrivals. The solid lines show the theoretical travel times calculated from the velocity model in Fig. 8.

tained by the line-up observations, the thickness of the upper layer can be estimated as 35–45 m.

We applied the time-term method of Merue (1966) to construct an initial velocity

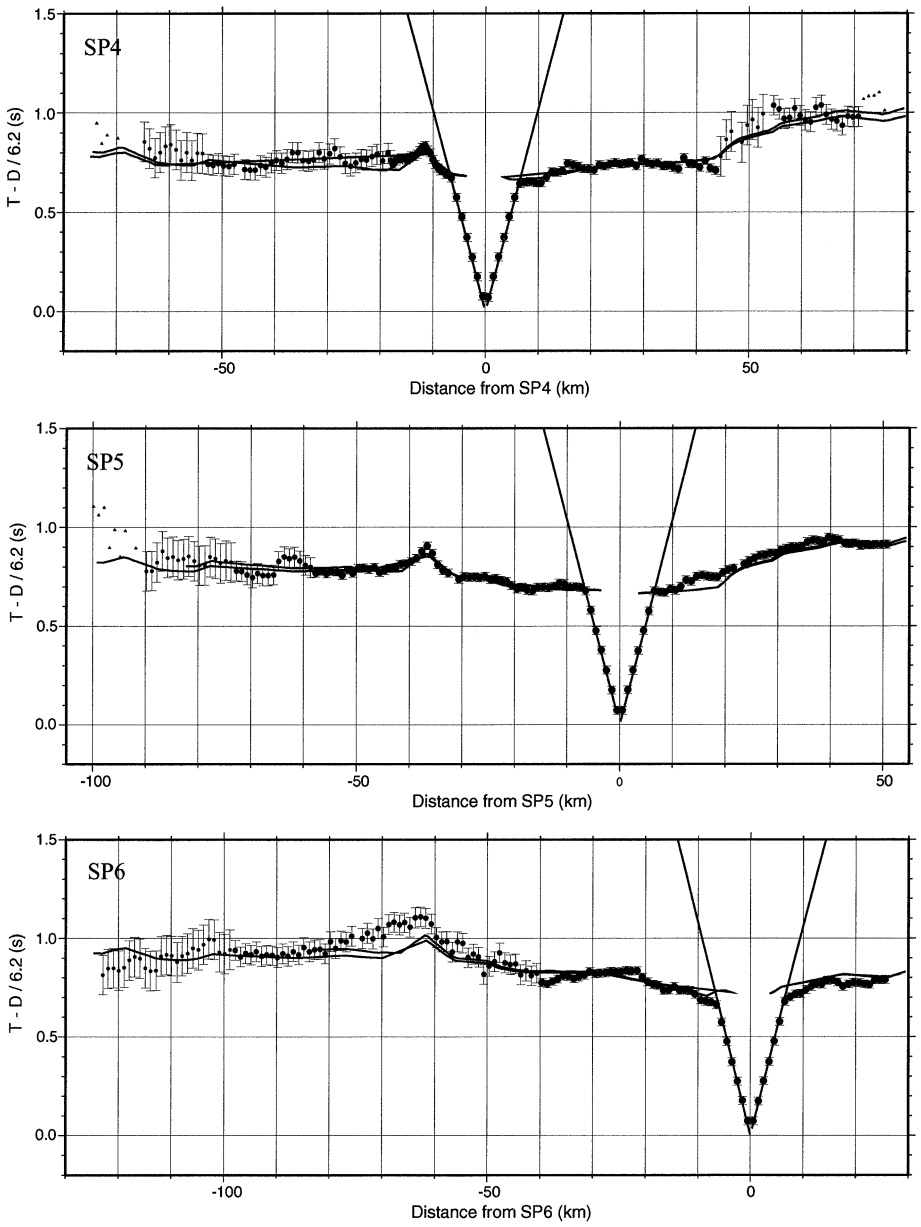

Fig. 4–2. Similar travel time plots for SP4, SP5 and SP6. Explanations are the same as in Fig. 4–1.

model for the ray tracing analysis. The estimated least squares velocity for the whole refracted waves at the bedrock is 6.09 km/s. However, the apparent velocity in the northern part is found to be different from that in the southern part. To obtain this local velocity distribution, we selected travel time data within the offset distance of 50 km for three adjacent shot points, and applied the method to the data. Figure 7 illustrates the result of the time-term analysis: the most probable velocities obtained are

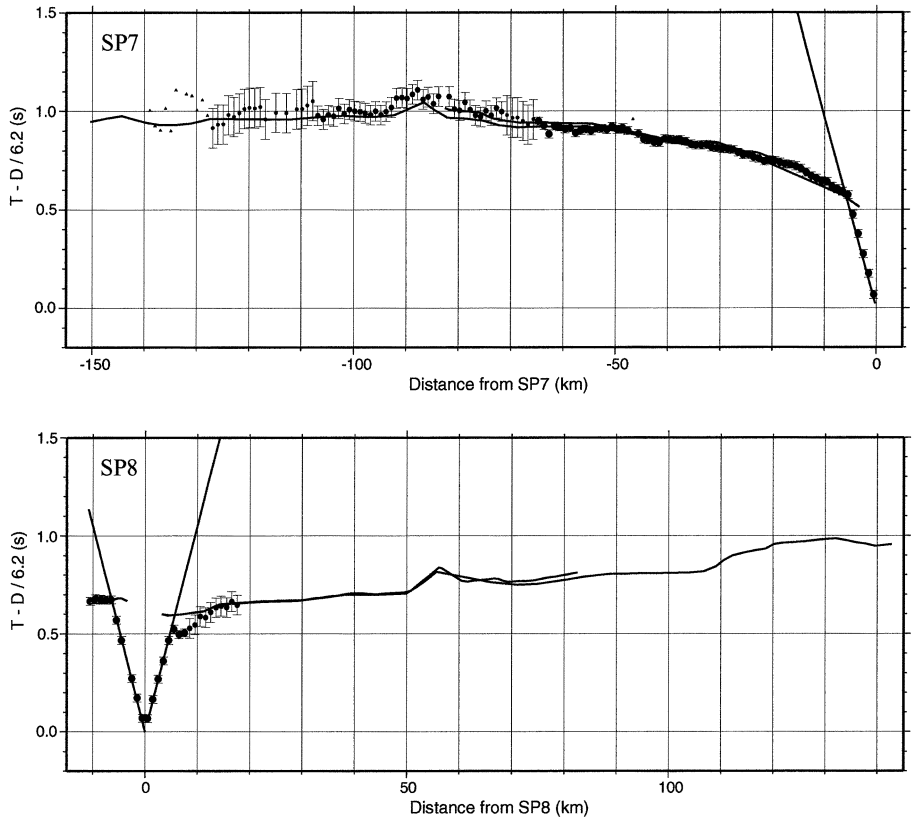

Fig. 4–3. Similar travel time plots for SP7 and SP8. Explanations are the same as in Fig. 4–1.

6.16 km/s (SP1 to SP3), 6.19 km/s (SP2 to SP4), 6.04 km/s (SP3 to SP5), 6.11 km/s (SP4 to SP6) and 5.94 km/s (SP5 to SP7), respectively. In summary, the most probable velocities obtained in the southern, central and northern parts are 6.2, 6.0–6.1 and 5.9 km/s, respectively. The depth distribution of the boundary between the ice sheet and the bedrock derived from the obtained time-terms is also presented in Fig. 7. As seen in the figure, it is noted that different combinations of the travel time data gave various time-term solutions.

Using the above results, we formulated an initial *P* wave velocity model. For simplicity, we disregarded the upper layer of the ice sheet of thickness 35–45 m and the *P* wave velocity of 2.7–2.9 km/s; the effect is negligibly small. Then, the *P* wave velocity for the whole ice sheet was assumed to be 3.7–3.9 km/s. We compared the observed travel time with the theoretical one calculated for the velocity model by a ray tracing procedure (Iwasaki, 1988), and adjusted the velocity parameters such as velocity distribution and boundary location by a trial-and-error procedure. We present the most suitable *P* wave velocity model in Fig. 8. Examples of the ray diagrams are shown in Fig. 9, and the theoretical travel times are drawn by thin solid lines in Fig. 4.

Characteristic features of the obtained model are summarized as follows: the *P* wave velocity of the ice sheet between SP1 and SP6 is about 3.8 km/s and that around

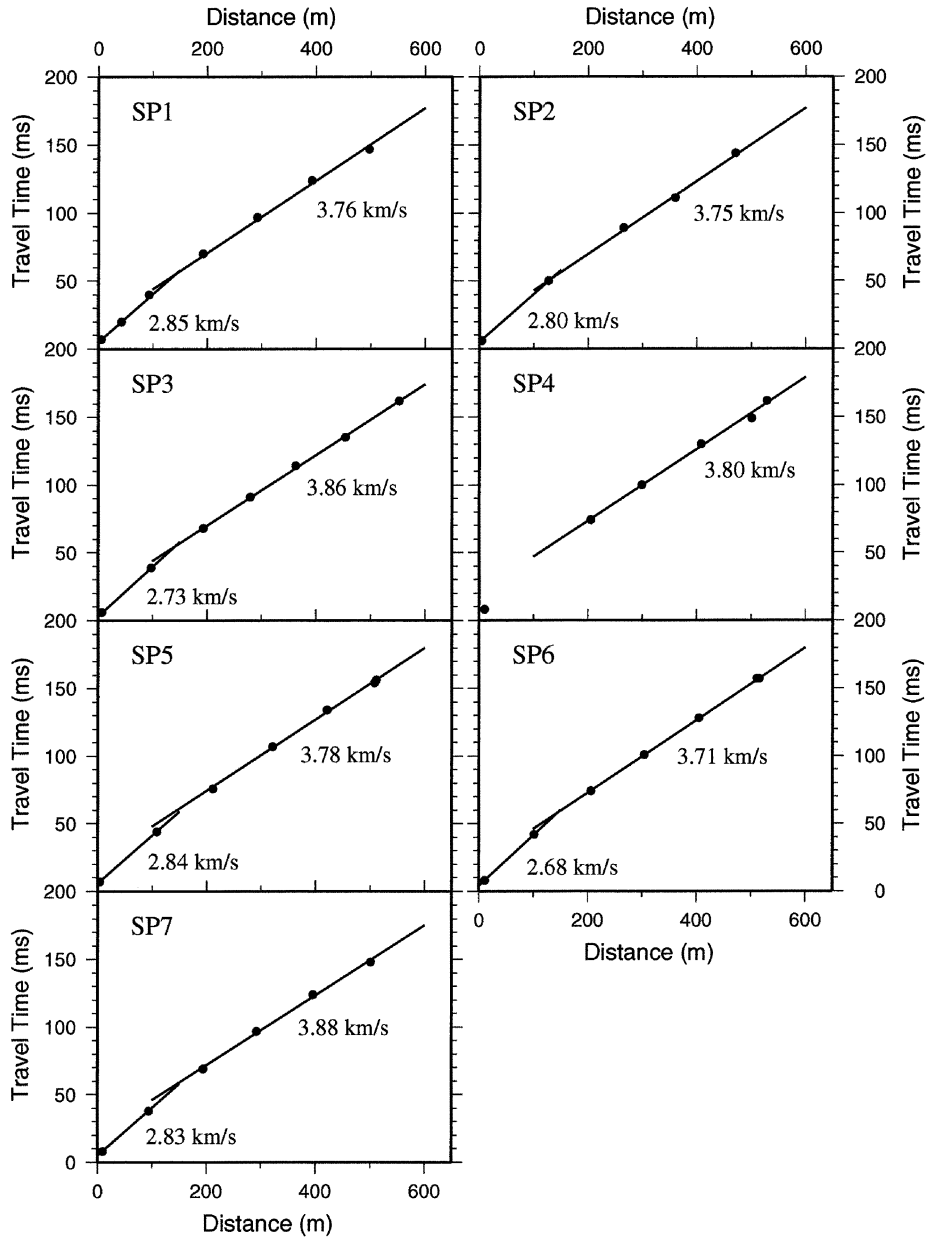

Fig. 5. P wave travel time plots obtained by the line-up observation for each shot. Numerals in the figure indicate the most probable velocities obtained by least squares analysis.

SP7 is 3.9 km/s, indicating that the velocities are faster in the low elevation area than in the high elevation area. A similar result was also obtained from the JARE-41 exploration (Miyamachi *et al.,* 2001; Tsutsui *et al.,* 2001a). The *P* wave velocity of the upper-most crust is found to have a lateral variation: the velocities are faster in the

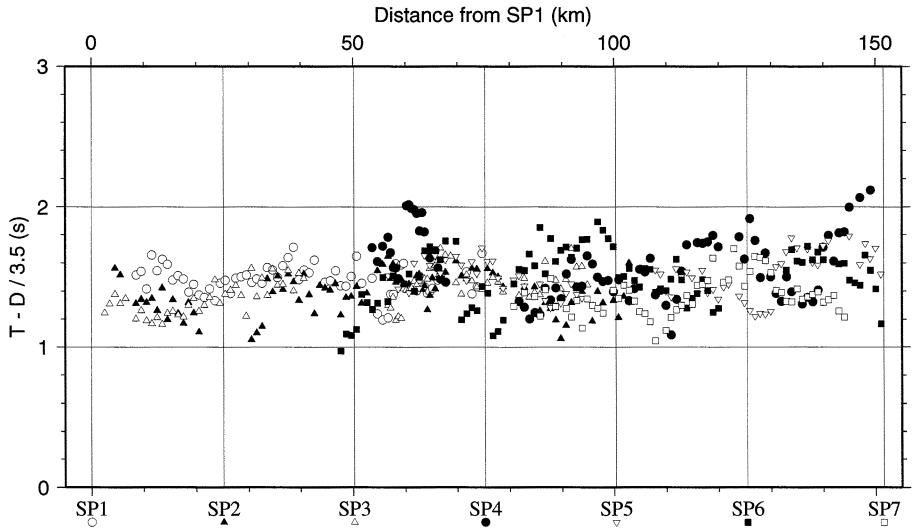

Fig. 6. S wave travel time plots reduced by the velocity of 3.5 km/s for SP1 to SP7. Each symbol corresponds to travel time data observed from each shot: open circles for SP1, solid triangles for SP2, open triangles for SP3, solid circles for SP4, inverted open triangles for SP5, solid squares for SP6 and open squares for SP7.

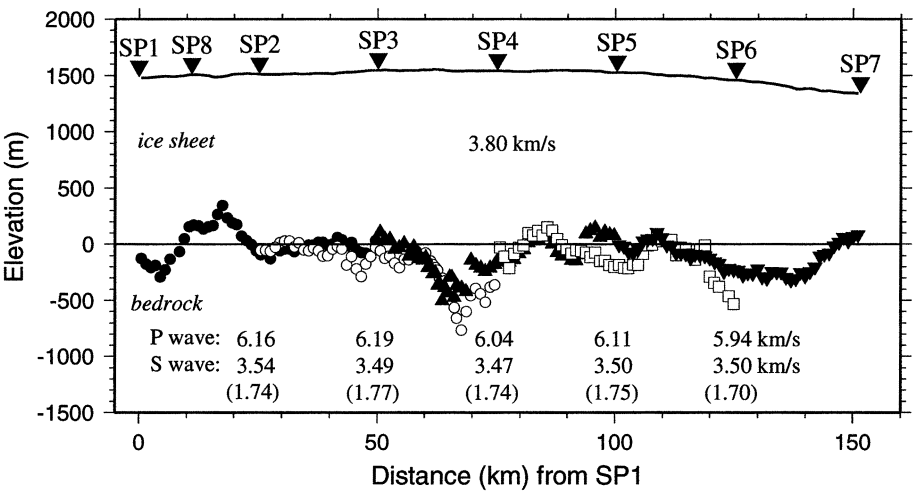

Fig. 7. Results of the time-term analysis. Symbols show the depths translated from the time-term solutions. Upper (P-wave) and lower (S-wave) numerals indicate the most probable velocities for the corresponding bedrock areas, respectively. Values in parentheses are the Poisson's ratio calculated from the P and S wave velocities.

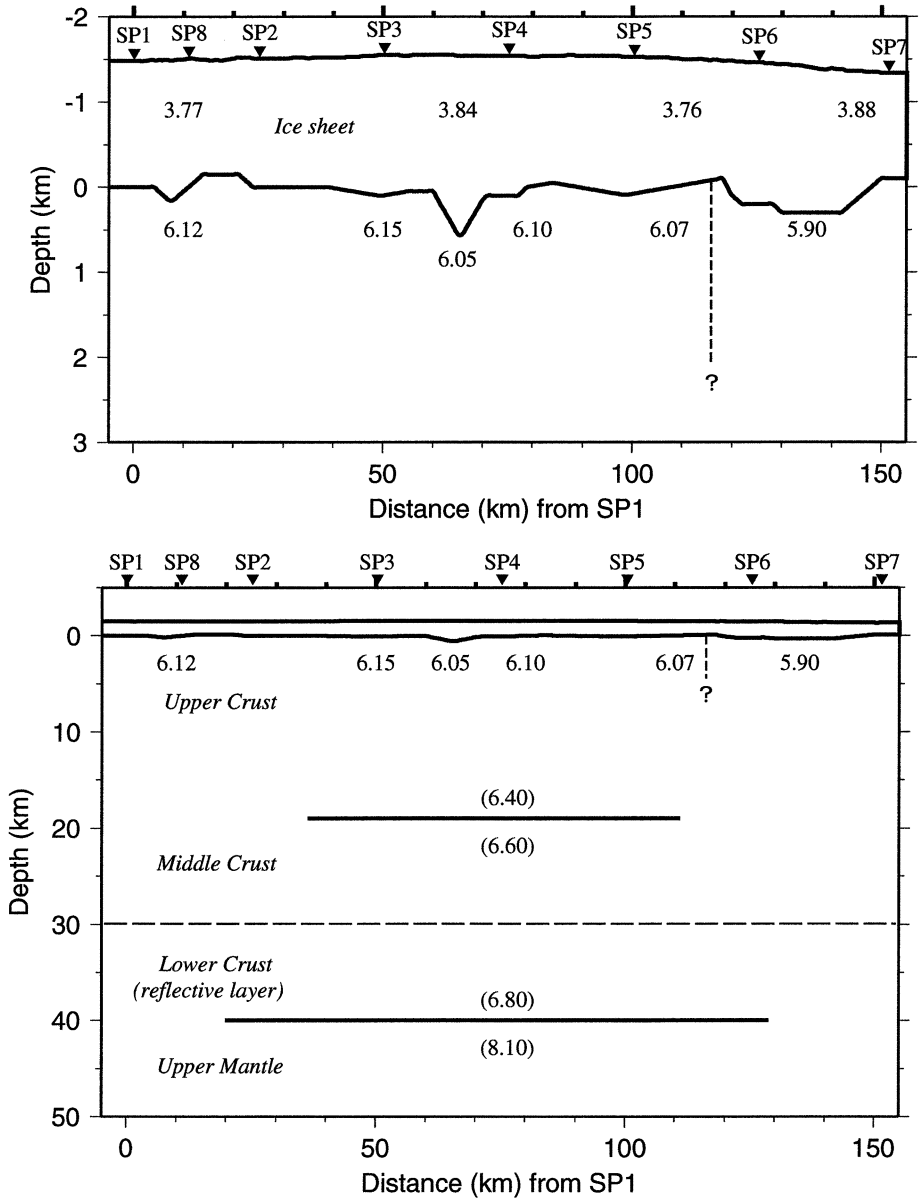

*Fig. 8. The velocity model estimated along the JARE-43 seismic line. Numerals in the figures are P wave velocities obtained by this study, and those within blankets are from Ikami et al. (1986) and Tsutsui et al. (2001a, b). Dashed vertical lines in the figures show the boundary estimated from the lateral velocity variation. The solid lines in the lower figure indicate the reflection planes estimated by the travel time analysis of the reflection phases "**R1**" and "**R2**".*

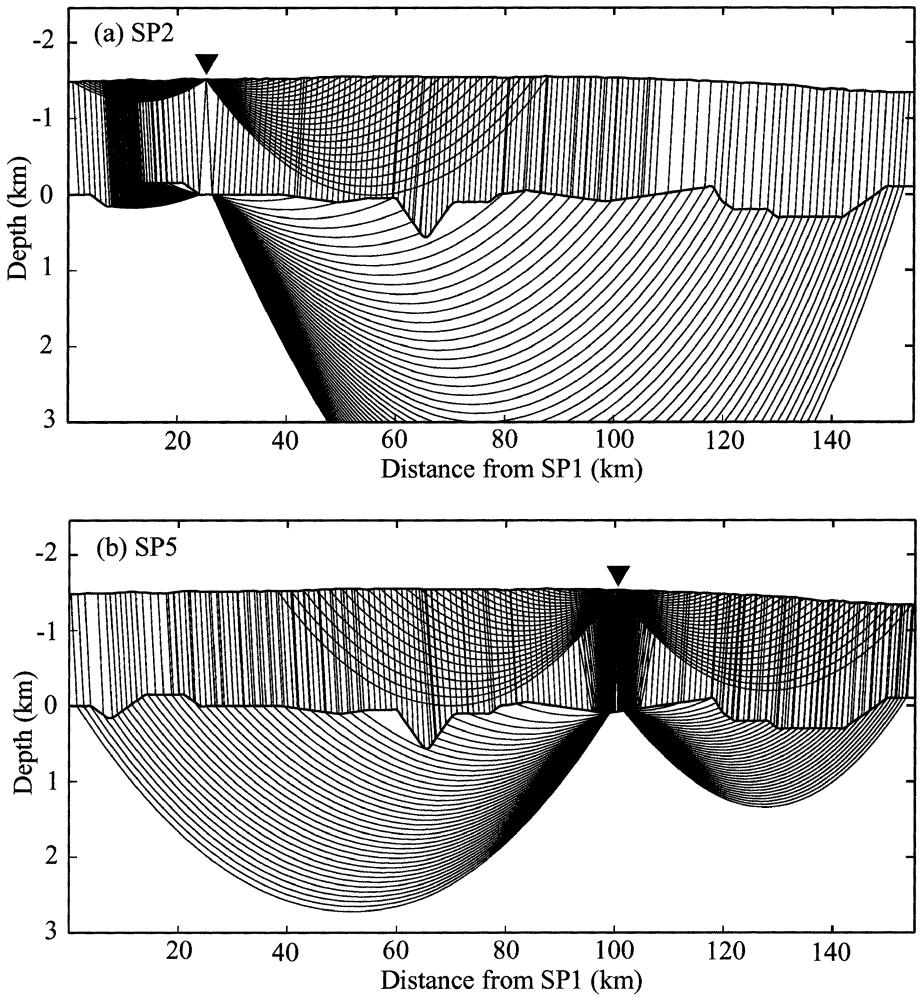

Fig. 9. Examples of the ray diagrams for SP2 and SP5 for the velocity model in Fig. 8.

southern and central parts (6.1–6.2 km/s) than in the northern part (5.9 km/s). As for the bedrock topography beneath the ice sheet, there is a steep valley with a height drop of about 600 m between SP3 and SP4, and the *P* wave velocity in the bottom area seems to be slower than that in the surrounding areas.

3.2. S wave refraction analysis

We estimated the most probable velocity by applying the time-term method to the *S* wave travel time data. The estimated least squares *S* wave velocity from the whole data set was 3.52 km/s. The data sets for adjacent three shot points provided most probable local velocities: they were 3.54 km/s (SP1 to SP3), 3.49 km/s (SP2 to SP4), 3.47 km/s (SP3 to SP5), 3.50 km/s (SP4 to SP6) and 3.50 km/s (SP5 to SP7) from southwest to northeast. Because of large errors in the travel time data, the lateral

variation indicated is not certain. From the local *P* and *S* wave velocities obtained independently in the time-term analysis, we estimated the *Vp/Vs* ratio as shown in the parentheses of Fig. 7: the ratio in the southern and central parts ranges from 1.74 to 1.77, which is larger than that of 1.70 in the northern part.

3.3. P wave wide-angle reflection analysis

To estimate the deep crustal structure, we direct our attention to two main reflection phases, labelled ***R1*** and ***R2***, in Fig. 3. Considering the previous studies by JARE-21, -22 and -41 (Ito and Ikami, 1984; Ikami *et al.,* 1984; Ikami and Ito, 1986; Tsutsui *et al.,* 2001a, b), we modeled the velocity profile in the middle and lower crust under the assumption that the reflection planes are horizontal. We estimated the depths of two reflecting planes by a travel time analysis using the ray tracing procedure. Figure 8 shows the obtained deep crustal model, and the reflecting planes corresponding to the reflections ***R1*** and ***R2*** are located at 19 and 40 km depths, respectively. It is reasonable that the phase ***R2*** is a PmP reflection associated with the Moho discontinuity.

The phases ***R3*** are found to arrive after about 0.6–0.7 s from the first onsets, and their distribution is parallel to the first onsets. Therefore, we presume that the phases ***R3*** are multiple-reflections in the ice sheet.

4. Discussion

4.1. Ice sheet

Ishizawa (1981) showed the *P* wave velocity in the ice sheet down to 100 m depth by a local seismic refraction experiment at Mizuho Station. According to his result, the *P* wave velocity increased rapidly down to 20 m depth and then reached 3.8 km/s at 100 m depth. We think that this steep gradient layer corresponds to our first layer with *P* wave velocity of 2.7–2.9 km/s. Tsutsui *et al.* (2001a) obtained a *P* wave velocity for the whole ice sheet of 3.8 km/s. The *P* wave velocity of 3.7–3.9 km/s in our study for the lower layer of the ice sheet is consistent with their results. As pointed out by Miyamachi *et al.* (2001), the gradual velocity increase in the lower layer may be due to the compaction effect of the ice sheet itself.

During the seismic exploration, we also carried out radio echo sounding along the northern and central parts of the seismic line to estimate the thickness of the ice sheet (Takada *et al.,* 2002). Figure 10 shows a comparison of the depth distributions of the ice sheet estimated by the radio echo sounding and the seismic exploration. As pointed out *e.g.* by Tsutsui *et al.* (2001a), radio echo sounding can reveal fine and local undulations of the depth distribution of the ice sheet. On the other hand, seismic waves with a wavelength of a few hundred meters reveal the longer undulations. Therefore, we believe that both results are consistent with each other in a spatially long wavelength undulation of the terrain.

The depth distribution of the ice sheet estimated by radio echo sounding is systematically (100 to 200 m) shallower than that observed by seismic exploration. This discrepancy is also reported in Tsutsui *et al.* (2001a). They discussed several possible reasons and finally concluded that the discrepancy was caused by a difference in the space resolution of the methods. Kanao *et al.* (1994) indicated the possible

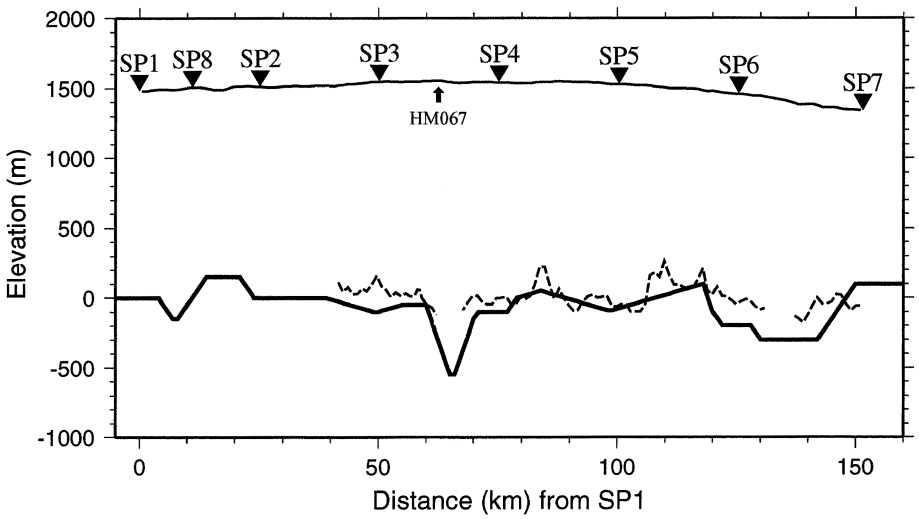

Fig. 10. Depth profile of the boundary between the ice sheet and the bedrock. Solid and dashed lines indicate the boundaries estimated by this study and by the radio echo sounding in Takada et al. (2002), respectively.

existence of a layer mixed by ice and moraine rocks over the bedrock. In this case, the radio waves are possibly reflected at the top of the mixed layer, while the seismic waves are refracted at the bottom of the layer, namely the top of the bedrock. Though our seismic data do not clearly detect the mixed layer, we think that this interpretation is reasonable.

Where the surface of the bedrock determined by seismic exploration is steeply inclined or valley-shaped, sufficient strength of the radio echo is not received. This may be possibly caused by two factors: first the radio wave transmitted vertically into the ice sheet did not return vertically to the receiver because of the steeply declined reflector, and second the bottom of the valley may be filled with an attenuating or scattering liquid. The relatively low velocity of the bedrock in the valley between SP3 and SP4 suggests this possibility. However, further studies will be required to solve this question.

4.2. Upper crustal structure

Tsutsui *et al.* (2001a) indicated that the *P* wave velocity for the upper-most crust was uniformly 6.2 km/s from the JARE-41 seismic survey. This velocity is consistent with the *P* wave velocity, 6.1–6.2 km/s, estimated for the central part of our seismic profile. They also show the possible layer with *P* wave velocity of 6.5 km/s at 5 km depth from a travel time analysis of the first onset over a distance range of more than 100 km. Because of the limited distance range of less than 100 km, we could not detect the corresponding layer.

The most remarkable result in our study is detection of the lateral velocity variation for the upper-most crust. The *P* wave velocity, 5.9 km/s, in the northern part is undoubtedly slower than that, 6.1–6.2 km/s, in the other parts. This result implies that

the material composing the upper-most crust of the northern part is different from that of the other parts, and the velocity boundary may be located between SP5 and SP6. The shape of the boundary remains to be determined.

Kanao *et al.* (1996) and Kanao (1997) obtained regional *S* wave velocity models down to 60 km depth in various areas of East Antarctica by receiver function inversion of broadband seismometer data. In their model, the *S* wave velocity in the upper-most crust in the Lützow-Holm Bay region ranges from 3.2 to 3.6 km/s. Considering the uncertainty of their result, our *S* wave velocity of 3.5 km/s must be more reliable.

4.3. Middle and lower crustal structure

The travel time analysis of the main reflection phases, ***R1*** and ***R2***, reveals the depths of two reflection planes to be 19 and 40 km, respectively. Ikami *et al.* (1984) showed the deep velocity model down to the Moho discontinuity at 40 km depth along the Mizuho route from the explosion experiments operated by JARE-21 and -22. In their model, the *P* wave velocity in the upper crust started from 6.0 km/s at sea level and gradually increased to 6.4 km at a depth of 13 km. A middle crust was shown to be composed of a layer with thickness of about 17 km and *P* wave velocity of 6.4 km/s. The thickness of the lower crust was about 10 km and the associated *P* wave velocity was 6.8–6.9 km/s. They also pointed out that the Conrad discontinuity at about 30 km depth may possibly be a transition zone with thickness of 2.4 km. Recently, Tsutsui *et al.* (2001b) revealed the detailed depth distribution of the Moho discontinuity from reflection analysis using the JARE-41 seismic data. The prominent feature is that the Moho discontinuity is inclined from the inland to the coast: its depth is 42 km beneath S-6 and 29 km beneath S-1 (see Fig. 1). According to their model, the depth of the Moho beneath our seismic line (H176 in Fig. 1) is expected to be 36–38 km, which is shallower than our result. This difference may be caused from velocity uncertainty in the middle and lower crust. We also examined the possibility of the inclined Moho discontinuity, but we concluded that it was not necessary to incline the Moho discontinuity beneath our seismic line.

Furthermore, we considered the reflection plane ***R1*** at 19 km depth from the SP2 and SP4 observations. There is no boundary corresponding to the plane ***R1*** in the model derived by Ikami *et al.* (1984). This may be due to too sparse station distribution to detect the reflection phases. On the other hand, the dense station distribution in JARE-41 by Tsutsui *et al.* (2001b) showed a reflection plane located at about 17 km depth, which can be identical with our plane ***R1***. From the reflection analysis, Ito and Kanao (1996) and Tsutsui *et al.* (2001b) also showed that the lower crust is a reflective layer with thickness of about 10 km.

4.4. Comparison with other geophysical and geological studies

Figure 11 shows the preliminary free-air and Bouguer anomaly distributions along the seismic line (Toda *et al.,* 2002). These gravity anomalies compensate for the effect of the thick ice sheet. Local undulation of the free-air anomaly is closely correlated with the depth distribution of the bedrock topography in Fig. 8. The negative Bouguer anomaly distribution in the whole profile may result from the thick crust. The relatively high Bouguer anomalies between SP3 and SP4 and between SP6 and SP7 are

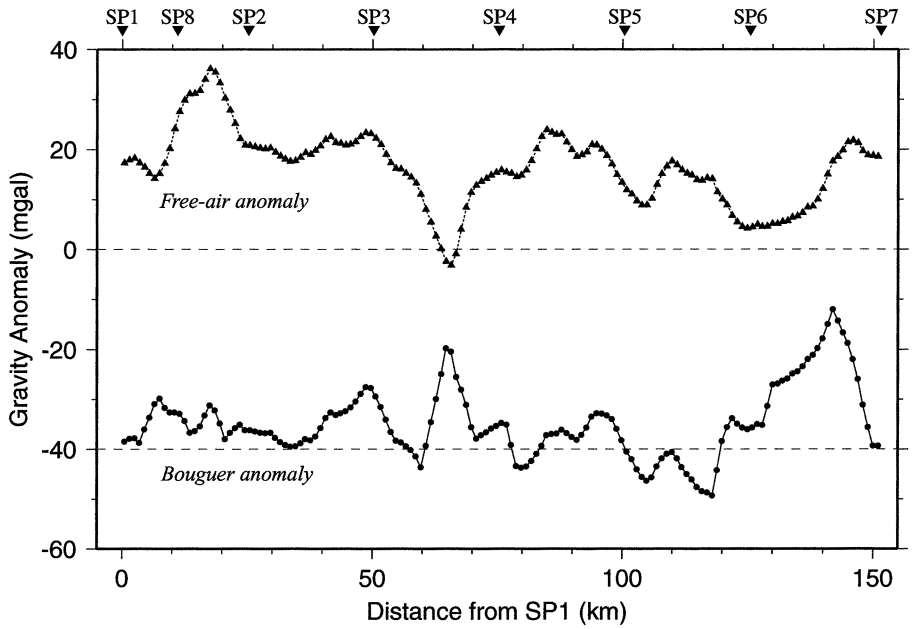

Fig. 11. Gravity anomaly distributions along the seismic line measured and calculated by Toda et al. (2002). Solid triangles and circles correspond to free-air and Bouguer anomalies, respectively.

considered to be apparent, due to an excessive correction in the Bouguer reduction calculated from the ice sheet distributed below the standard elevation, namely 0 m in the WGS84 ellipsoidal height (Toda *et al.,* 2002). Except for these areas, the Bouguer anomaly in the area from SP1 to SP5 is generally greater than −40 mgal. On the other hand, the anomaly between SP5 and SP6 is less than −40 mgal; this supports the existence of a velocity boundary which is inferred from the lateral *P* wave velocity variation.

We determined the local velocity variation in the upper-most crust. From geological observations along coastal regions of Enderby Land and Dronning Maud Land in East Antarctica, Hiroi *et al.* (1991) presented the metamorphic rock facies distribution in the Paleozoic Lützow-Holm Complex. As shown in Fig. 1, they pointed out that the metamorphic grade increased from the amphibolite-granulite facies transition zone to the granulite facies zone along the NE–SW direction in the Lützow-Holm Bay region. In general, the *P* wave velocity of the granulite facies rock is relatively faster than that of the amphibolite facies rock, because of higher density of the granulite facies rock than the relatively lower density of the amphibolite facies rock (Rudnick and Fountain, 1995). Therefore, the southern and central parts of our seismic profile with *P* wave velocity of 6.1–6.2 km/s can be considered as corresponding to the granulite facies zone, while the northern part with *P* wave velocity of 5.9 km/s corresponds to the transition zone. Accordingly, the geological boundary observed on the coast may possibly extend to the inland area between SP5 and SP6. In addition, we presume that the fluctuation of the *P* wave velocity distribution for the upper-most crust obtained in the central and

southern parts may reflect the metamorphic grade and/or rock compositions of the amphibolite-granulite facies in the Lützow-Holm Complex.

Shingai *et al.* (2001) measured *P* wave velocities in ultrahigh temperature granulite rocks sampled from the Napier Complex, East Antarctica. They suggested that the Lützow-Holm Complex spread out over the Napier Complex on the Mizuho Plateau: the upper and the middle crusts are composed of the Lützow-Holm Complex and the Napier Complex, respectively. The reflection plane ***R1*** at 19 km depth may possibly correspond to the boundary between the Lützow-Holm Complex (the upper crust) and the Napier Complex (the middle crust).

5. Conclusions

The JARE-43 seismic exploration consisted of 7 large shots, 1 small shot and 161 seismic stations configured on the 151 km-long seismic line, on the Mizuho Plateau, East Antarctica. The travel time analysis revealed the detailed *P* wave velocity distribution of the ice sheet and the upper-most crust. The *P* wave velocity of the thin first layer of the ice sheet is 2.7–2.8 km/s and that of the second layer, which continues down to the bedrock, is 3.8 km/s. The depth of the bedrock is almost at sea level. The *P* wave velocity of the upper-most crust in the northern part is 5.9 km/s and that in the central and southern parts is 6.1–6.2 km/s; this lateral variation implies that the metamorphic rock facies of the Lützow-Holm Complex along the coast extends to the inland area. We also obtained the average *S* wave velocity as 3.5 km/s in the upper-most crust. The analysis of the prominent reflection phase revealed that the Moho discontinuity is at 40 km depth. The other reflection plane at 19 km depth may possibly correspond to the boundary between the Lützow-Holm Complex and the Napier Complex.

Finally, it is proved that seismic exploration is very useful to investigate geological features, especially in an area where the thick ice sheet covers the crust such as Antarctica. Therefore, it is important to conduct further seismic explorations in the Antarctic region to understand the evolution of the continental crust.

Acknowledgments

We would like to express our special appreciation to participants in this exploration: Y. Takahashi, D. Kamiya, M. Yanagisawa, N. Ishizaki, K. Nakano, T. Nakamura, N. Yoshida, T. Yasuhara and K. Horiguchi. We are grateful to members of JARE-43 (led by F. Nishio and K. Kamiyama), members of JARE-42 (led by Y. Motoyoshi) and the crew of the icebreaker "*Shirase*" (captain Y. Ishikado). We give special thanks to Prof. K. Shibuya and other staff members of the National Institute of Polar Research. Thanks also go to Prof. K. Moriwaki and two anonymous referees for improving the manuscript.

References

Hiroi, Y., Shiraishi, K. and Motoyoshi, Y. (1991): Late Proterozoic paired metamorphic complexes in East Antarctica, with special reference to the tectonic significance of ultramafic rocks. Geological

Evolution of Antarctica, ed. by M.R.A. Thomson *et al.* Cambridge, Cambridge Univ. Press, 83–87.
Ikami, A. and Ito, K. (1986): Crustal structure in the Mizuho Plateau, East Antarctica, by a two dimensional ray approximation. J. Geodyn., **6**, 271–283.
Ikami, A., Ito, K., Shibuya, K. and Kaminuma, K. (1984): Deep crustal structure along the profile between Syowa and Mizuho Stations, East Antarctica. Mem. Natl Inst. Polar Res., Ser. C, **15**, 19–28.
Ishizawa, K. (1981): The measurement of the velocities of *P* and *S* waves propagating in the surface layer of ice sheet at Mizuho Station, East Antarctica. Nankyoku Shiryô (Antarct. Rec.), **73**, 147–160.
Ito, K. and Ikami, A. (1984): Upper crustal structure of the Prince Olav Coast, East Antarctica. Mem. Natl Inst. Polar Res., Ser. C, **15**, 13–18.
Ito, K. and Kanao, M. (1996): Detection of reflected waves from the lower crust on the Mizuho Plateau, East Antarctica. Nankyoku Shiryô (Antarct. Rec.), **39**, 233–242.
Iwasaki, T. (1988): Ray-tracing program for study of velocity structure by ocean bottom seismographic profiling. Zishin (J. Seismol. Soc. Jpn.), **41**, 263–266 (in Japanese).
Kanao, M. (1997): Variations in the crust structure of the Lüzow-Holm Bay region, East Antarctica using shear wave velocity. Tectonophysics, **270**, 43–72.
Kanao, M. (2001): Crustal evolution and deep structure viewed from East Antarctic Shield, "Structure and Evolution of the East Antarctic Lithosphere Geotransect Project" —Outline and scientific significance—. Bull. Earthq. Res. Inst., Univ. Tokyo, **76**, 3–12 (in Japanese with English abstract).
Kanao, M., Kamiyama, K. and Ito, K. (1994): Crustal density structure of the Mizuho Plateau, East Antarctica from gravity survey in 1992. Proc. NIPR Symp. Antarct. Geosci., **7**, 23–36.
Kanao, M., Kubo, A. and Shibutani, T. (1996): Crustal velocity models of shear waves in East Antarctica by receiver function inversion of broadband waveforms. Proc. NIPR Symp. Antarct. Geosci., **9**, 1–15.
Merue, R.F. (1966): An iterative method for solving the time-term equation. The Earth Beneath the Continent, ed. by J.S. Steinhart and T.J. Smith. Washington, Am. Geophys. Union, 495–497 (AGU Monograph **10**).
Miyamachi H., Murakami, H., Tsutsui, T., Toda, S., Minta, T. and Yanagisawa, M. (2001): A seismic refraction experiment in 2000 on the Mizuho Plateau, East Antarctica (JARE-41)—outline of observations—. Nankyoku Shiryô (Antarct. Rec.), **45**, 101–147 (in Japanese with English abstract).
Miyamachi, H., Toda, S., Matsushima, T., Takada, M., Takahashi, Y., Kamiya, D., Watanabe, A., Yamashita, M. and Yanagisawa M. (2003): A seismic refraction and wide-angle reflection exploration in 2002 on the Mizuho Plateau, East Antarctica—outline of observations (JARE-43)—. Nankyoku Shiryô (Antarct. Rec.), **47**, 32–71 (in Japanese with English abstract).
Rudnick, R.L. and Fountain, D.M. (1995): Nature and composition of the continental crust: a lower crustal perspective. Rev. Geophys., **33**, 267–309.
Shingai, E., Ishikawa, M. and Arima, M. (2001): *P*-wave velocity in ultrahigh temperature granulites from the Archean Napier Complex, East Antarctica. Polar Geosci., **14**, 165–179.
Shiraishi, K., Ellis, D.J., Hiroi, Y., Fanning, C.M., Motoyoshi, Y. and Nakai, Y. (1994): Cambrian orogenic belt in East Antarctica and Sri Lanka; Implications for Gondwana assembly. J. Geol., **102**, 47–65.
Takada, M., Toda, S., Kamiya, D., Maeno, H., Matsuoka, K., Miyamachi, H., Kanao, M. and Furukawa, T. (2002): Radio echo sounding survey on the Mizuho Plateau in the SEAL Project, the JARE 43rd (2002), East Antarctica. The 22nd Symposium on Antarctic Geosciences, Program and Abstract. Tokyo, Natl Inst. Polar Res., 78–79 (in Japanese).
Toda, S., Kamiya, D., Takada, M., Matsushima, T., Miyamachi, H., Kanao, M. and Fukuda, Y. (2002): GPS and gravity surveys on the Mizuho Plateau in the SEAL Project, the JARE 43rd (2002), East Antarctica. The 22nd Symposium on Antarctic Geosciences, Program and Abstract. Tokyo, Natl Inst. Polar Res., 81–82 (in Japanese).
Tsutsui, T., Murakami, H., Miyamachi, H., Toda, S. and Kanao, M. (2001a): *P*-wave velocity structure of the ice sheet and the shallow crust beneath the Mizuho traverse route, East Antarctica, from seismic refraction analysis. Polar Geosci., **14**, 195–211.
Tsutsui, T., Yamashita, M., Murakami H., Miyamachi, H., Toda, S. and Kanao M. (2001b): Reflection profiling and velocity structure beneath Mizuho traverse route, East Antarctica. Polar Geosci., **14**, 212–225.